Piezo-Thermal Conductivity Effect in Germanium

R. W. KEYES* AND R. J. SLADEK†
Westinghouse Research Laboratories, Pittsburgh, Pennsylvania
(Received August 30, 1961)

The effect of static elastic strain on the thermal conductivity of germanium has been measured in the temperature interval 1.5° to 4.2°K. A large increase in thermal conductivity was produced by [111] or [110] tension in antimony-doped samples in which the scattering of phonons is primarily due to donors. The theory of scattering of phonons by donors predicts the sign and magnitude of the effect. Samples without strong donor scattering show small piezo-thermal conductivity effects.

INTRODUCTION

RECENT experiments[1–3] show that the thermal resistance of germanium at low temperatures is greatly increased by the presence of antimony donors. The thermal resistance due to donors exhibits some interesting features in addition to its large magnitude: the thermal conductivity increases with temperature more rapidly than T^3 at low temperatures and the effect is much larger for antimony than for arsenic donors.[2,3] In a previous paper,[4] hereafter referred to as I, it was shown that these unusual features can be understood as resulting from the large effects of the elastic strain produced by the phonons on the donor wave functions.[5,6] The considerations developed in I led us to anticipate a large effect of static elastic strain on the thermal conductivity of antimony-doped germanium at low temperatures. Our investigation of this piezo-thermal conductivity effect is reported in the present paper.

EXPERIMENTAL DETAILS

The potentiometric form of the axial flow method for measuring thermal conductivity[7] was used. Thermal insulation of the specimen was complicated by the need to apply stress to it. Consequently, the calorimeter part of the apparatus was constructed as shown in Fig. 1. Some of its essential features will be pointed out and discussed briefly below.

The specimen is suspended in a can which can be evacuated to a pressure of $\leq 10^{-7}$ mm Hg. Nylon cords are used in the suspension near the specimen so that pure tension can be applied. One piece of nylon connects the bottom grip on the specimen to a fitting on the beryllium-copper yoke. Another piece of nylon connects the heater-grip on the top end of the specimen to a radiation shield and thereby to the stress transmitting wire. The other end of this wire is connected to one arm of a lever whose fulcrum is a high-vacuum-tight, ball joint. The other arm of the level supports a tray for holding weights.

The thermal circuit will now be traced. Heat generated electrically in the heater flows down through the sample and lower grip to a silver wire (0.032-in. diam) and thereby to the liquid helium bath. The silver wire is needed to complete the thermal circuit because of the high thermal resistance of the nylon cord connecting the lower sample grip to the yoke. Most of the thermal resistance downwards from the heater to the bath is in the sample for the samples of lowest thermal conductivity but not for the others. Consequently, the lowest sample temperature achieved for the lowest bath temperature of 1.2°K depended on the sample being measured. Since the silver wire presumably has less thermal resistance than even the purest Ge sample, most of the thermal resistance must have occurred at the solder joints between sample and grips and between the bottom grip and the silver wire. Additional thermal resistance at the lower end of the silver wire was avoided since this end of the wire ran through a hole in the can (where it was soldered in place to preserve the vacuum integrity).

In order that the heat current through the sample be equal to the electrical power dissipated in the heater, it is necessary that heat flow down the pull wire system to the sample be negligible compared to the heater power. To accomplish this, the pull wire was made of low-thermal conductance material—stainless steel type 302 of 0.030-in. diam—but more important, it was heat-stationed as follows: A number of staggered radiation shields were attached to it, and the lower two of these shields were put into thermal contact with the helium bath by means of an annealed, highest-purity, silver wire (0.032-in. diam). The end of this silver wire was brought through a hole in the pumping tube and soldered in place to preserve the vacuum integrity. Heat flow from the heater upwards to the bath via the heat-stationed pull wire was negligible because of the high-thermal resistance provided

---

* Present address: IBM Research Center, Yorktown Heights, New York.
† Present address: Department of Physics, Purdue University, Lafayette, Indiana.
[1] E. Fagen, J. Goff, and N. Pearlman, Phys. Rev. 94, 1415 (1954).
[2] J. F. Goff and N. Pearlman, Bull. Am. Phys. Soc. 4, 410 (1959).
[3] J. F. Goff and N. Pearlman, in *Proceedings of the Seventh International Conference on Low-Temperature Physics, Toronto, 1960* (University of Toronto Press, Toronto, 1961), p. 284.
[4] R. W. Keyes, Bull. Am. Phys. Soc. 5, 264 (1960); Phys. Rev. 122, 1171 (1961).
[5] P. J. Price, Phys. Rev. 104, 1223 (1956).
[6] H. Fritzsche, Phys. Rev. 115, 336 (1959).
[7] G. K. White, *Experimental Techniques in Low-Temperature Physics* (Clarendon Press, Oxford, 1959), p. 154.

mainly by the nylon cord and connections near the sample.

The temperature gradient and mean temperature in the sample were determined from two carbon resistor thermometers which were calibrated for every low temperature run against the vapor pressure of the bath with He exchange gas in the can and no current flowing in the heater. Without the exchange gas, the resistors indicated temperatures which were only very slightly higher (~0.002°K). This provides evidence for the effectiveness of the heat-stationing discussed above.

The electrical leads to the thermometers and the heater were brought out of the can into the bath through a kovar-glass multi-terminal seal to prevent heat flow down them to the sample. Thermal shorting of the sample to the bath due to these leads was avoided by making them of small diameter (0.002 in.) manganin. To keep Joule heat from developing in these leads due to heater or thermometer current, they had a thin coating of PbSn solder which is superconducting at the temperatures of our measurements.

The carbon resistor thermometers were constructed of 12-ohm, 1/10-watt, Allen-Bradley resistors as follows. The insulation was removed from the resistors and they were cemented into close-fitting copper sleeves from which they were insulated by a layer of 0.5-mil paper. To improve thermal contact between the resistor and its sleeve, one lead of the resistor was connected via a short copper wire (0.010-in. diam) to the sleeve. The copper sleeves were connected to the sample by about $\frac{1}{8}$ in. of 0.010-in. diam copper wire, soldered to the sleeve at one end and to the sample at the other. The small area of contact to the sample thus provided should isolate the thermometers from the strain applied to the sample and thus avoid any change in their calibration due to such strain. Evidence for adequate isolation from the strain is twofold: (1) application of stress to the sample during calibration of the thermometers did not affect the calibration, and (2) no piezo-thermal conductivity effect was observed in samples where it is not expected, e.g., pure n-type germanium. The values of some experimental parameters were as follows:

Heater power—0.013 mw to 4 mw.
Temperature differences—0.02°K to 0.10°K.
Thermometer resistances—~52 ohms at 4.2°K to ~300 ohms at 1.3°K.
Thermometer measuring current—14 μa to 100 μa.
Thermometer calibration accuracy—±0.001°K.
Bath temperature control—±0.0005°K or better.

Samples

All but one of the samples were obtained from single-crystal germanium ingots grown in this laboratory by the Czochralski method. They were cut by means of a diamond wheel perpendicular to the growth direction to minimize the gradient in impurity concentration along the length of the sample. The other sample was zone-leveled. Good homogeneity of the thermal conductivity samples was indicated by Hall measurements made at room or liquid nitrogen temperatures on samples which were obtained from the ingots immediately adjacent to where the thermal conductivity samples were obtained. Hall coefficients for different sets of leads on a given sample agreed within 10%.

The thermal conductivity samples to be reported on were lapped and etched with CP-4 etch to dimensions of about 0.1 cm×0.2 cm×2.5 cm. Etched samples broke less radily than lapped ones, hence, their use. The samples were soldered into copper grips which extended about 0.3 cm along the sample from each end. The carbon thermometers were located about 1 cm apart around the center of the sample. Characteristics of the samples are given in Table I.

In addition to the above samples, a lapped sample of pure n-Ge (from material adjacent to that which provided sample 5n) was also measured. Comparison

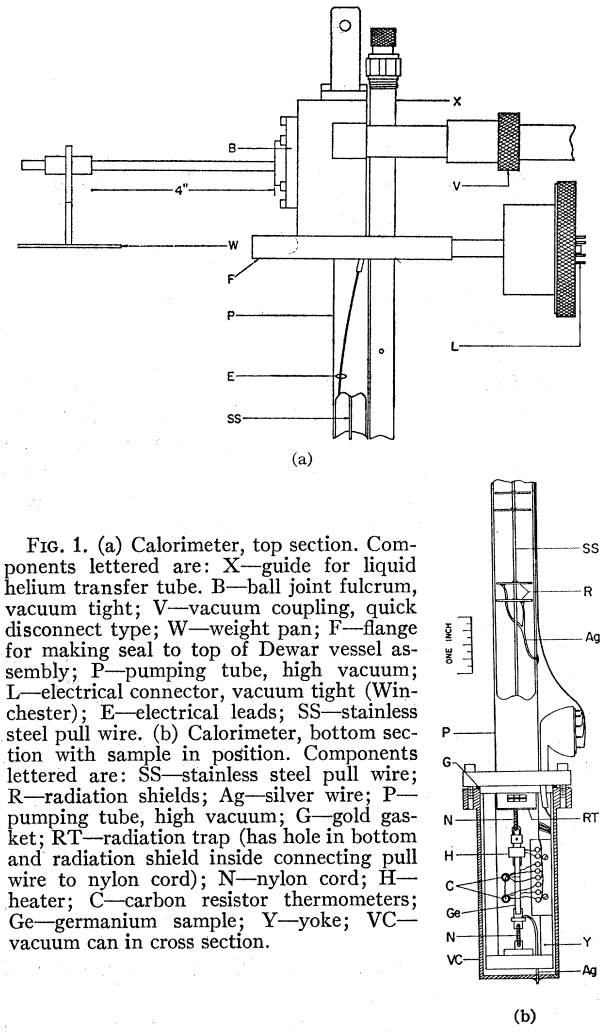

FIG. 1. (a) Calorimeter, top section. Components lettered are: X—guide for liquid helium transfer tube. B—ball joint fulcrum, vacuum tight; V—vacuum coupling, quick disconnect type; W—weight pan; F—flange for making seal to top of Dewar vessel assembly; P—pumping tube, high vacuum; L—electrical connector, vacuum tight (Winchester); E—electrical leads; SS—stainless steel pull wire. (b) Calorimeter, bottom section with sample in position. Components lettered are: SS—stainless steel pull wire; R—radiation shields; Ag—silver wire; P—pumping tube, high vacuum; G—gold gasket; RT—radiation trap (has hole in bottom and radiation shield inside connecting pull wire to nylon cord); N—nylon cord; H—heater; C—carbon resistor thermometers; Ge—germanium sample; Y—yoke; VC—vacuum can in cross section.

TABLE I. Properties of the samples used in the piezo-thermal conductivity experiment.

Sample	Orientation	ρ(300°K) ohm cm	n cm^{-3}	Impurity	W(2.5°K) w^{-1} cm deg	Effect of strain on thermal conductivity
1n	[110]	0.13	2×10^{16}	Sb	3.8	Large increase
2n	[111]	0.12	2×10^{16}	Sb	3.8	Large increase
3n	[100]	0.20	1×10^{16}	Sb	2.2	No effect
4n	[110]	0.12	2×10^{16}	As	1.05	$\lesssim$10% increase
5n	[111]	31	...	...	0.61	No effect
1P	[110]	47	...	...	0.64	15% decrease

of the results with those on sample 5n confirmed the observations of Geballe[8] that the scattering of phonons by boundaries in pure germanium may be completely diffuse in lapped samples and may be as much as 50% specular in etched samples. This corresponds to the phonon mean free path in etched samples being over twice the sample width. Recently Toxen[9] has found a smaller degree of specularity for boundary scattering (20%) in a sample of Ge etched with CP-4.

RESULTS

The essential features of the results are summarized in the last column of Table I and in Figs. 2 and 3. The samples can readily be divided into two classes: (1) Those in which there is a large effect of strain on the thermal conductivity in the liquid helium temperature range (a stress of 10^8 dynes/cm^2 increases the thermal conductivity by a factor two or more at very low temperatures). (2) Those in which the effect of strain is always less than 20% (again for a stress of 10^8 dynes/cm^2). The last column of Table I indicates the class to which each sample belongs. Figures 2 and 3 are plots of thermal conductivity vs temperature for samples with no applied stress and with applied stresses of about 10^8 dynes/cm^2.

Figure 4 shows the stress dependence of the thermal resistivity at selected temperatures for the samples which show a large piezo-thermal conductivity effect. The accuracy is not sufficient to give good values for the initial slopes of the thermal resistivity versus stress curves. The curve for the lowest temperature seems to be approaching a limiting value at high stresses. This limiting value is still about five times the thermal resistivity of pure Ge.

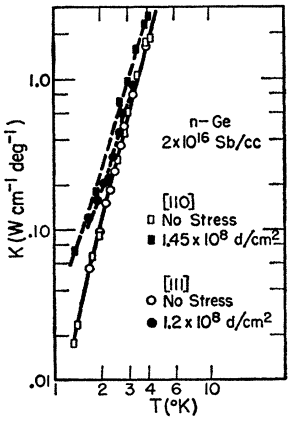

FIG. 2. Thermal conductivity versus temperature of Ge samples showing large changes in thermal conductivity due to tensile stress.

THEORY AND INTERPRETATION

It is apparent that the results are in qualitative accord with the effects which we anticipated on the basis of the model presented in I. According to this model the scattering of phonons by a donor is very sensitive to the detailed nature of the ground electronic state of the donor. The composition of the lowest donor state can be radically changed by elastic strain, however.[5,6,10–12] The wave function of the state is derived in equal proportions from all four valleys in the unstrained crystal. Strain increases the contribution to the wave function of those valleys which are lowered in energy by the strain. This change in the electronic composition of the ground state can be expected to produce a change in the scattering of phonons by the donor. A comparison between the observed piezo-thermal conductivity effects and the detailed predictions of our model will be presented in this section.

First, it should be noted that a large effect of strain is to be expected only in those two samples in which it is found. In the pure samples there are so few donors that scattering by them is negligible, and boundary scattering dominates. In the arsenic-doped sample, scattering by donors is weaker than in the antimony-doped sample, and in addition, the effect of strain on the donor wave function is much smaller for an arsenic donor than for an antimony donor.[6] In the antimony-doped samples, tension in a [100] directions does not change the donor wave functions, while tension in [110] and [111] direction does. Thus, a large change in phonon scattering is to be expected only in the latter samples. This orientation dependence of a piezo-thermal conductivity effect is to be expected on the basis of any model which attributes the scattering of phonons to electrons, since a strain with a [100] axis does not remove the degeneracy of [111] valleys, and is not characteristic of the particular mechanism of electronic scattering considered in I.

[8] T. H. Geballe, J. Appl. Phys. 30, 1153 (1959).
[9] A. M. Toxen, Phys. Rev. 122, 450 (1961).
[10] G. Weinreich, W. S. Boyle, H. G. White, and K. F. Rodgers, Phys. Rev. Letters 2, 96 (1959).
[11] D. K. Wilson and G. Feher, Bull. Am. Phys. Soc. 5, 60 (1960).
[12] R. W. Keyes and P. J. Price, Phys. Rev. Letters 5, 473 (1960).

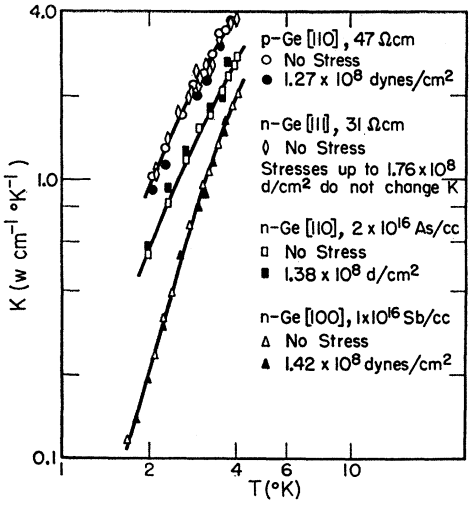

FIG. 3. Thermal conductivity versus temperature of Ge samples showing little or no change in thermal conductivity due to tensile stress.

The large size of the piezo-thermal conductivity effects shown in Figs. 2 and 4 can be accounted for by the donor scattering model. According to the model, the composition of the donor state could be changed completely by a strain, ϵ, which shifted the valley energies by the amount of the chemical shift, 4Δ.[5] This strain is roughly determined by $\Xi_u\epsilon=4\Delta$, where Ξ_u is the shear deformation potential constant. Since $\epsilon=X/C_{44}$, where X is the stress, the strain which changes the thermal resistance by an amount of the same order as the thermal resistance itself is $X\approx 4\Delta C_{44}/\Xi_u=2\times 10^7$ dyne/cm^2 for antimony donors. This estimate adequately accounts for the very large observed magnitude of the piezo-thermal conductivity. It is strong support for the model of I, since it is difficult to see how a model which did not involve a comparison of the effect of strain on the valley energies with the chemical shift could give rise to such a large piezo-thermal conductivity. The effect is smaller for arsenic donors since the critical strain is about an order of magnitude larger in this case because of the large value of 4Δ for arsenic.

The details of the sign, magnitude and character of the piezo-thermal conductivity effects pose a more difficult problem. A theory of the phonon relaxation times in strained germanium can be worked out in close analogy with the method described in I. The calculation, however, is much more complicated because of the reduced symmetry of the problem. In addition, even if the results for the phonon relaxation time are obtained, the calculation of the thermal conductivity involves additional difficulties which were not resolved in an entirely satisfactory way in I. Therefore, we have not pursued this program to its end. For interpretation of our data, it is instructive, nevertheless, to examine the expressions for the second order perturbation of the energy which give rise to the scattering of phonons, i.e., the formulas analogous to Eq. (2.3) of I for strained germanium.

Let the axis along which the static tension is applied (the sample axis in our experimental arrangement) be defined by the unit vector $\mathbf{b}$ and the magnitude of the applied stress be X. Then the change in the energy of valley (i) produced by the shear component of the static stress is

$$u^{(i)}=(\Xi_u X/2C_{44})[(\mathbf{a}^{(i)}\cdot\mathbf{b})^2-\tfrac{1}{3}], \qquad (1)$$

where $\mathbf{a}^{(i)}$ is a unit vector along the [111] type axis of valley (i). The dilatational component of the stress does not affect the composition of the donor states and will not be considered here.

[111] Stress

When $\mathbf{b}=[1,1,1]/\sqrt{3}$, the Hamiltonian which determines the energy levels of the $1s$-like donor states in the presence of the strain defined by Eq. (1) is[5]

$$\mathcal{H}=\begin{vmatrix} u^{(1)}+3\rho\Delta & -\Delta & -\Delta & -\Delta \\ -\Delta & u^{(2)}-\rho\Delta & -\Delta & -\Delta \\ -\Delta & -\Delta & u^{(3)}-\rho\Delta & -\Delta \\ -\Delta & -\Delta & -\Delta & u^{(4)}-\rho\Delta \end{vmatrix}. \qquad (2)$$

Here the zero of energy has been chosen as the energy of a hydrogen-like state in the "decoupled" approximation.[5] The quantity $u^{(i)}$ is the displacement of the energy of the "decoupled" state arising from valley

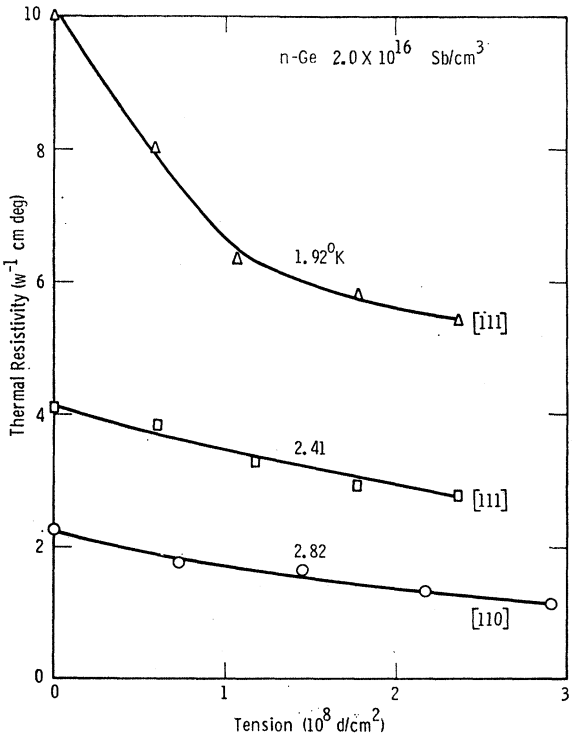

FIG. 4. Thermal resistivity versus tension at three different temperatures for Ge samples as indicated.

(i) by the strain other than the applied static strain given by Eq. (1). In the present problem the strain which gives rise to the $u^{(i)}$ is that due to the phonons. The calculation of the $u^{(i)}$ is described in more detail in I, in particular, by Eq. (2.2) of I. The quantity ρ in Eq. (2) is a measure of the displacement of the valley energies by the static strain Eq. (1). It has the value

$$\rho=\Xi_u X/9C_{44}\Delta. \tag{3}$$

Following I, we diagonalize $\mathcal{H}$, Eq. (2), with respect to Δ and the effects of the static strain, then use second-order perturbation theory to expand the energy of the lowest state of the donor to second order terms in the $u^{(i)}$. We obtain for these second-order terms

$$E_2=-(3/64\Delta)F_L(\rho)[u^{(1)}-\tfrac{1}{3}(u^{(2)}+u^{(3)}+u^{(4)})]^2 -(1/24\Delta)F_T(\rho)[u^{(4)2}+u^{(2)2}+u^{(3)2} -u^{(2)}u^{(3)}-u^{(3)}u^{(4)}-u^{(4)}u^{(2)}]. \tag{4}$$

Here

$$F_L(\rho)=\gamma^{-3}, \tag{5}$$

$$F_T(\rho)=(2/3\gamma)(1+2\rho+2\gamma)/(1-\rho+\gamma), \tag{6}$$

where $\gamma\equiv(1+\rho+\rho^2)^{\frac{1}{2}}$. The functions F_L and F_T are plotted in Fig. 5. As in I, the quadratic terms in the energy Eq. (4) are the source of the scattering of the phonons.

[110] Stress

When the static stress is applied in the [110] direction the Hamiltonian corresponding to Eq. (2) is[5]

$$\mathcal{H}=\begin{vmatrix} u^{(1)}+2\sigma\Delta & -\Delta & -\Delta & -\Delta \\ -\Delta & u^{(2)}+2\sigma\Delta & -\Delta & -\Delta \\ -\Delta & -\Delta & u^{(3)}-2\sigma\Delta & -\Delta \\ -\Delta & -\Delta & -\Delta & u^{(4)}-2\sigma\Delta \end{vmatrix}. \tag{7}$$

Here the quantity σ is a measure of the displacement of the valley energies by the static strain Eq. (1). It has the value

$$\sigma=\Xi_u X/12C_{44}\Delta. \tag{8}$$

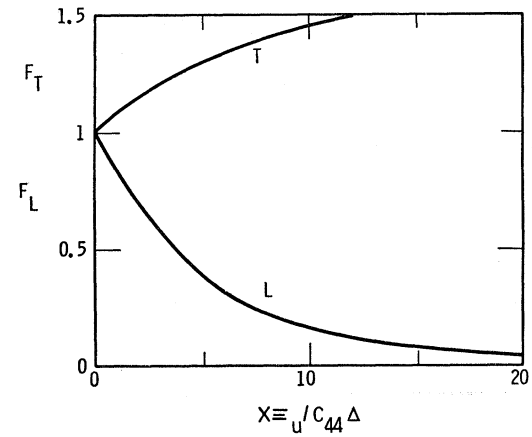

FIG. 5. The functions $F_L(\rho)$ and $F_T(\rho)$ defined by Eqs. (5) and (6). The stress unit, $C_{44}\Delta/\Xi_u$, has the value 5×10^6 dyne/cm² for antimony donors and 3.5×10^7 dyne/cm² for arsenic donors.

Again we expand the energy of the lowest state of the donor to second order terms in the $u^{(i)}$ and obtain for the quadratic terms

$$E_2=-(1/64\Delta)[G_L(\sigma)(u^{(1)}+u^{(2)}-u^{(3)}-u^{(4)})^2 +2G_{T2}(\sigma)(u^{(1)}-u^{(2)})^2+2G_{T1}(\sigma)(u^{(3)}-u^{(4)})^2]. \tag{9}$$

Here

$$G_L(\sigma)=(1+\sigma^2)^{-\frac{3}{2}}, \tag{10}$$

$$G_{T1}(\sigma)=2[1+\sigma(1+\sigma^2)^{-\frac{1}{2}}]/[(1+\sigma^2)^{\frac{1}{2}}-\sigma+1], \tag{11}$$

$$G_{T2}(\sigma)=2[1-\sigma(1+\sigma^2)^{-\frac{1}{2}}]/[(1+\sigma^2)^{\frac{1}{2}}+\sigma+1], \tag{12}$$

The functions $G_L(\sigma)$, $G_{T1}(\sigma)$, and $G_{T2}(\sigma)$ are plotted in Fig. 6.

Thermal Conductivity

As already mentioned, we shall not attempt to carry out a complete calculation of the thermal conductivity with scattering due to the perturbations given by the above equations. However, we recognize that those phonons with propagation vectors close to the sample axis will make the largest contribution to the thermal conductivity. Thus we may hope to get a rough idea of the effect of strain on the thermal resistance by evaluating its effect on the phonons with wave vector **q** parallel to **b**, the sample axis.

Considering first the [111] case, it is found that the scattering of longitudinal phonons with **q** parallel to [111] comes from the first term of Eq. (4), and the scattering of transverse phonons with this **q** comes from the second term of Eq. (4). Consequently, an estimate of the way in which the scattering of the longitudinal and transverse modes which contribute to the thermal conductivity is changed by the strain is given by the functions $F_L(\rho)$ and $F_T(\rho)$, Eqs. (5) and (6), respectively. It is then seen from Fig. 5 that F_L and hence the scattering of longitudinal waves decreases with increasing strain and disappears at large values of strain. The function F_T and hence the scattering of transverse waves increases slightly with strain. Since the conductivities due to the longitudinal and transverse phonons are essentially in parallel, the conductivity contribution which increases with strain will dominate, and the total thermal conductivity will be increased by strain.

The qualitative basis of this result is as follows: The longitudinal phonons are scattered by shifting of the energy of valley (1), the [111] valley, with respect to the average energy. However, the strain due to a longitudinal phonon propagating in the [111] direction is identical in crystallographic orientation to the static strain. Since, when the static strain is large, the energy is a linear function of the static strain, the perturbation due to the phonons contains no quadratic term. Therefore, it does not cause scattering of the phonons.

Considering next the [110] case, the scattering of longitudinal phonons propagating in the [110] direction comes from the term in Eq. (9) which is proportional

to $G_L(\sigma)$, the scattering of [110][1$\bar{1}$0] phonons comes from the term proportional to $G_{T1}(\sigma)$, and the scattering of [110][001] phonons comes from the term proportional to $G_{T2}(\sigma)$. Figure 6 shows that $G_L(\sigma)$ and $G_{T2}(\sigma)$ approach zero for large stress. The disappearance of the scattering of the longitudinal phonons occurs for essentially the same reason as in the [111] case. The vanishing of the scattering of the $T2$ phonon is a matter of detail; it is due to the fact that the $T2$ phonon is scattered by interaction with the valleys which are raised in energy by the [110] tensile stress, and are consequently removed from the wave function of the lowest donor state.[5] The function G_{T1} increases with increasing strain, and is four times larger in the high strain limit than at zero strain. However, as shown in I, the theory predicts no scattering of the $T1$ phonon because of the vanishing of the term in the $u^{(i)}$ in Eq. (9) for this phonon. As discussed in I, the difficulty of treating this feature of the phonon scattering was an unsatisfactory aspect of the calculation of thermal resistance presented there. In any case, it is seen that the present calculation predicts no scattering for any of the phonons propagating in a [110] direction in the large strain limit. Thus, it is also expected in this case that the thermal conductivity will be increased by the strain.

According to the above discussion, the thermal resistivity due to scattering of phonons by Sb donors in [111] and [110] samples should vanish almost completely at large strain. This implies that the thermal resistance of these samples should approach that of pure Ge at large strain. Experimentally, this is far from being true as we already noted in discussing Fig. 4. Such a discrepancy is not surprising since the discussion given above deals with only those phonons for which the effect of stress is a maximum.

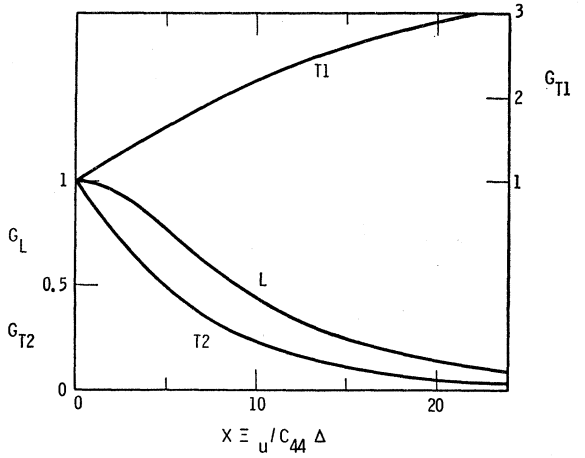

FIG. 6. The functions $G_L(\sigma)$, $G_{T1}(\sigma)$, and $G_{T2}(\sigma)$, defined by Eqs. (10)–(12). The stress unit, $C_{44}\Delta/\Xi_u$, has the value 5×10^6 dyne/cm^2 for antimony donors and 3.5×10^7 dyne/cm^2 for arsenic donors.

CONCLUSIONS

The experimental results are in reasonable qualitative agreement with the predictions of the donor scattering model. The order of magnitude, sign, and crystallographic character of the piezo-thermal conductivity effects are correctly given by the theory in those samples in which donor scattering is strong. The piezo-thermal conductivity effect is small in those samples in which donor scattering is absent or weak.

ACKNOWLEDGMENTS

Thanks are due to D. Watt for help with most of the experiment and for crystal growing, to J. Albrecht for design and construction of the ball-joint fulcrum and for construction of other parts of the apparatus, and to G. Wagner for helping with the measurements.